Gold Nanoparticles Bearing an α-Lipoic Acid-based Ligand Shell: Synthesis, Model Complexes and Studies Concerning Phosphorescent Platinum(II)-Functionalisation

Ulrich Siemeling[a], Frauke Bretthauer[a], Clemens Bruhn[a], Tim-Patrick Fellinger[b], Wah-Leung Tong[c], and Michael C. W. Chan[c]

[a] Institut für Chemie, Universität Kassel, Heinrich-Plett-Straße 40, 34132 Kassel, Germany
[b] Max-Planck-Institut für Kolloid- und Grenzflächenforschung, Am Mühlenberg 1, 14476 Potsdam, Germany
[c] Department of Biology and Chemistry, City University of Hong Kong, Tat Chee Avenue, Kowloon, Hong Kong SAR, China

Reprint requests to Prof. Dr. Ulrich Siemeling. Fax: +49 561 804 4777.
E-mail: siemeling@uni-kassel.de

Z. Naturforsch. **2010**, *65b,* 1089 – 1096; received March 31, 2010

The surface functionalisation of gold nanoparticles (GNPs) with luminescent platinum complexes has been investigated, utilising α-lipoic acid derivatives for GNP stabilisation. Model complexes have been studied to mimic the chemisorption chemistry required to afford GNPs protected by an α-lipoic acid-based ligand shell with terminal functionalisation suitable for metal coordination, and the unambiguous binding of the cyclic disulfide moiety at a zero-valent precious metal core through oxidative addition has been confirmed by X-ray crystallography. Subsequently, gold nanoparticles bearing the α-lipoic acid-based ligand shell have been prepared and characterised, and a synthetic methodology for the immobilisation of Pt^{II} luminophores onto their surface has been established.

Key words: Gold, Luminescence, Nanoparticles, Platinum, Self-assembly

Introduction

Functionalised monolayer-protected gold nanoparticles are useful for a wide range of applications [1 – 9]. The surface functionalisation of gold nanoparticles (GNPs) with metal complexes is of particular current interest and represents a burgeoning field in this regard [10 – 15]. We have developed an interest in gold nanoparticles functionalised with phosphorescent Pt^{II} complexes in the ligand shell. While chromophore-functionalised gold nanoparticles which contain organic fluorophores are well known [16, 17], phosphorescent metal-containing analogues are scarce [18 – 20]. Pt^{II} complexes (especially those based on tridentate chelate ligands) have been widely investigated as phosphorescent sensors, since the square-planar coordination environment of Pt^{II} allows axial interaction with guest molecules, which leads to changes in the local environment of the luminophore and can induce profound photoluminescence responses [21 – 23].

We have focused our efforts on Pt^{II} chelates containing tridentate cyclometallated C^N^N ligands (C^N^N = 6-*o*-arylene-2,2′-bipyridine, Fig. 1), which

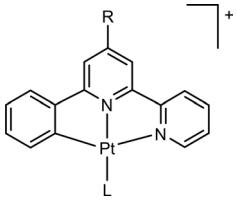

Fig. 1. Pt^{II} chelates with tridentate cyclometallated C^N^N ligands relevant to our study.

have been utilised as sensors for the recognition and detection of, *inter alia*, DNA, proteins and volatile organic compounds [24 – 28]. The luminescence properties of complexes bearing one or more Pt^{II}(C^N^N) luminophores are strongly dependent on weak Pt···Pt and π-π interactions, which can occur intramolecularly or between adjacent molecules in a preorganised environment, and switching between emission from the ^{3}MLCT state (λ_{em} *ca.* 550 – 600 nm) to low-energy emission from the ^{3}MMLCT state ($\lambda_{em} > ca.$ 650 nm) can be induced by guest species which perturb these weak interactions [29, 30]. In the present context the preorganised environment may be provided by the self-assembled ligand shell surrounding a monolayer-protected gold nanoparticle. Phosphorescence quench-

ing by the gold nanoparticle is expected to be of minor significance, since the energy of the plasmon absorption band ($\lambda_{max} \leq 521$ nm for particles ≤ 22 nm) [31] is considerably higher than that of the low-energy emission band of the chosen Pt^{II} luminophores.

Experimental Section

Synthetic work involving air-sensitive compounds was performed under an atmosphere of dry nitrogen by using standard Schlenk techniques or a conventional glovebox. Solvents (including those for photophysical measurements) were dried and purified according to standard methods. [PtCl(C^NPh^N)] (C^NPh^N = 4-phenyl-6-*o*-phenylene-2,2′-bipyridine) was prepared according to a published procedure [30]. All other chemicals were procured from standard commercial sources and used as received. ^{1}H NMR spectra were recorded on Varian Unity INOVA 500 or Bruker DRX 400 FT-NMR spectrometers (ppm) using Me_4Si as internal standard, and ^{13}C NMR spectra were recorded on the latter of the two instruments. IR spectra were recorded with Bio-RAD FTS-40A or Perkin-Elmer 1600 series FT-IR spectrophotometers (ATR mode, if not stated otherwise). High-resolution ESI mass spectra were obtained with a micrOTOF instrument (Bruker Daltonics, Bremen, Germany) utilising an Apollo^{TM} ion funnel ESI ion source. Mass calibration was performed immediately prior to the measurement with ESI Tune Mix Standard (Agilent, Waldbronn, Germany). Standard ESI mass spectra were measured on a Perkin-Elmer Sciex API 365 mass spectrometer. TEM studies were performed with a Zeiss EM 10 C transmission electron microscope at 60 or 80 eV, utilising carbon-coated copper grids (Formvar®, Plano GmbH, Wetzlar, Germany). TEM data analyses were performed with the programs IMAGEJ and GWYDDION. Elemental analyses were carried out by the microanalytical laboratory of the University of Kassel, or on an Elementar Analysensysteme GmbH Vario EL elemental analyser. UV/Vis absorption spectra were obtained on an Agilent 8453 diode array spectrophotometer. Steady-state emission spectra were recorded on a SPEX FluoroLog 3-TCSPC spectrophotometer equipped with a Hamamatsu R928 PMT detector. Sample solutions were degassed with at least three freeze-pump-thaw cycles. X-Ray crystal structure analyses: For each data collection a single crystal was mounted on a glass fibre, and all geometric and intensity data were taken from this sample. Data collection using MoK_α radiation (λ = 0.71073 Å) was made on a Stoe IPDS2 diffractometer equipped with a 2-circle goniometer and an area detector. Absorption correction was done by integration using X-RED [32]. The data sets were corrected for Lorentz and polarisation effects. The structures were solved by Direct Methods (SHELXS-97) and refined using alternating cycles of least-squares refinements against F^2 (SHELXL-97) [33]. All non-H atoms were found in difference Fourier maps and were refined with anisotropic displacement parameters. H atoms were placed in constrained positions according to the riding model with the 1.2-fold isotropic displacement parameters. The solvent molecules present in **2**·3.5C_6H_6 have been included in the model with constrained hexagonal symmetry. Pertinent crystallographic data are collected in Table 1. Graphical representations were made using ORTEP-3 WIN [34].

Table 1. Crystal data and structure refinement for compounds **1** and **2**·3.5C_6H_6.

Compound	**1**	**2**·3.5C_6H_6
Empirical formula	$C_{13}H_{18}N_2OS_2$	$C_{70}H_{69}N_2OP_2PtS_2$
Formula weight	282.41	1275.42
Temperature, K	153(2)	143(2)
Crystal system	monoclinic	triclinic
Space group	$P2_1/c$	$P\bar{1}$
a, Å	8.8635(14)	10.2582(13)
b, Å	13.9845(16)	14.003(3)
c, Å	11.6558(14)	23.073(3)
α, deg	90	80.960(13)
β, deg	90.737(11)	79.510(11)
γ, deg	90	71.567(12)
Cell volume, Å^3	1444.6(3)	3074.2(8)
Z	4	2
$d_{calc.}$, g cm^{-3}	1.30	1.38
μ, mm^{-1}	0.4	2.4
$F(000)$	600	1302
θ range, deg	2.30 to 24.99	1.45 to 25.23
Index ranges	$-10 \leq h \leq 10$	$-12 \leq h \leq 12$
	$-12 \leq k \leq 16$	$-16 \leq k \leq 16$
	$-13 \leq l \leq 12$	$-27 \leq l \leq 26$
Refls. collect. / indep.	5191 / 2438 /	20133 / 10308 /
R_{int}	0.0988	0.1759
Refls. observed	1157	2965
T_{min} / T_{max}	0.9201 / 0.9955	0.5622 / 0.8253
Data / restraints / params	2438 / 0 / 166	10308 / 0 / 262
Final indices $R1$ /	0.0700 /	0.0825 /
$wR2$ [$I \geq 2\sigma(I)$]	0.1742	0.1540
Final indices $R1$ /	0.1355 /	0.2227 /
$wR2$ (all data)	0.1999	0.1954
GOF on F^2	0.905	0.722
Largest diff. peak /	0.514	1.811
hole, e Å^{-3}	−0.326	−1.730

CCDC 746851–746852 contain the supplementary crystallographic data for this paper. These data can be obtained free of charge from The Cambridge Crystallographic Data Centre *via* www.ccdc.cam.ac.uk/data_request/cif.

*Preparation of lip-C(O)NH-py (**1**)*

HOBt (656 mg, 4.85 mmol) was added to a stirred solution of α-lipoic acid (1.00 g, 4.85 mmol), 4-aminopyridine (456 mg, 4.85 mmol) and EDCCl (296 mg, 5.34 mmol) in dichloromethane (50 mL). After 65 h the mixture was washed with water (4 × 50 mL) and dried with $CaSO_4$. Volatile components were removed *in vacuo*, affording the

crude product as a light-yellow solid which was dissolved in a minimum amount of ethyl acetate and purified by column chromatography (silica gel, ethyl acetate-*n*-hexane 4 : 1). Yield 548 mg (40 %). – ^{1}H NMR ($CDCl_3$): δ = 1.49 (m, 2 H), 1.70 (m, 4 H), 1.89 (m, 1 H), 2.37 (m, 3 H), 3.10 (m, 1 H), 3.16 (m, 1 H), 3.56 (m, 1 H), 7.51 (m, 2 H), 7.79 (s, 1 H), 8.46 (m, 2 H). – IR: ν(C=O) 1697, ν(C-C_{arom}) 1590, ν(C-N) + δ(N-H) 1521 cm^{-1}. – HRMS ((+)-ESI): *m/z* = 283.09333 (calcd. 283.09388 for $C_{13}H_{19}N_2OS_2$, $[M+H]^+$). – Anal. for $C_{13}H_{18}N_2OS_2$ (282.4): calcd. C 55.29, H 6.42, N 9.92; found C 55.44, H 6.22, N 9.90.

Preparation of the Pt^{II} chelate ***2***

A 5 mm NMR tube was charged with $[Pt(PPh_3)_4]$ (50 mg, 0.04 mmol) and **1** (11 mg, 0.04 mmol), and C_6D_6 (2 mL) was added. The solution was investigated by ^{31}P NMR spectroscopy, which indicated that the reaction was essentially complete after *ca.* 6 h; yield (NMR) quantitative. After 12 h the solution was carefully layered with *n*-hexane to induce crystallisation. Light-orange single crystals suitable for an X-ray diffraction study were obtained after several days. ^{1}H NMR (C_6D_6): δ = 1.15 (m, 1 H), 1.27 (m, 2 H), 1.49 (m, 2 H), 1.60 (m, 1 H), 1.95 (m, 1 H), 2.23 (m, 2 H), 3.10 (m, 1 H), 3.19 (m, 1 H), 7.25 (m 36 H), 7.55 (m, 2 H), 7.60 (s, 1 H), 8.4 (m, 2 H). – ^{31}P NMR (C_6D_6): δ = 23.7 (d, J_{pp} = 20.5 Hz), 26.2 (d, J_{pp} = 20.5 Hz).

*Preparation of lip-C(O)NH-Ph (****3****)*

Aniline (452 mg, 4.85 mmol) was added to a solution of α-lipoic acid (1.00 g, 4.85 mmol), DCC (1.00 g, 4.85 mmol) and HOBt (655 mg, 4.85 mmol) in dichloromethane (30 mL). After 72 h the precipitate was filtered off. The filtrate was reduced to dryness *in vacuo*, affording the crude product as a light-yellow solid, which was purified by column chromatography (silica gel, dichloromethane-methanol 30 : 1). Yield 519 mg (38 %). – ^{1}H NMR ($CDCl_3$): δ = 1.51 (m, 2 H), 1.73 (m, 4 H), 1.90 (m, 1 H), 2.36 (m, 2 H), 2.45 (m, 1 H), 3.10 (m, 1 H), 3.17 (m, 1 H), 3.57 (m, 1 H), 7.09 (m, 1 H), 7.19 (s, 1 H), 7.30 ("d", apparent *J* = 7.9 Hz, 2 H), 7.49 ("d", apparent *J* = 8.0 Hz, 2 H). – IR: ν = 1655, 1597, 1533 cm^{-1}. – HRMS ((+)-ESI): *m/z* = 282.09880 (cald. 282.09863 for $C_{14}H_{20}NOS_2$, $[M+H]^+$). – Anal. for $C_{14}H_{19}NOS_2$ (281.4): calcd. C 59.75, H 6.80, N 4.98; found C 60.19, H 7.42, N 4.98.

*Preparation of [Pt(****1****)(C^NPh^N)]PF$_6$ (****4****)*

A suspension of [PtCl(C^NPh^N)] (31 mg, 0.058 mmol) and **1** (19 mg, 0.067 mmol) in CH_3CN/CH_3OH (1 : 1, 12 mL) was refluxed for 48 h to give a clear orange solution. The solution was filtered into methanolic $[NH_4][PF_6]$ (47 mg, 0.29 mmol), which gave a yellow precipitate upon cooling. The precipitate was collected and washed with diethyl ether. Recrystallisation by diffusion of diethyl ether into a CH_3CN solution afforded a yellow crystalline solid. Yield 34 mg (75 %). – ^{1}H NMR (CD_3CN): δ = 1.48 – 1.55 (m, 2 H), 1.63 – 1.79 (m, 4 H), 1.91 – 1.97 (m, 1 H), 2.48 (m, 3 H), 3.11 – 3.23 (m, 2 H), 3.61 – 3.68 (m, 1 H), 6.43 (m, 1 H), 7.08 (m, 2 H), 7.59 (m, 4 H), 7.66 (m, 1 H), 7.80 (d, *J* = 7.0 Hz, 2 H), 7.86 (m, 2 H), 7.94 (s, 1H), 8.03 (d, *J* = 4.7 Hz, 1 H), 8.06 (s, 1 H), 8.21 (m, 1 H), 8.29 (d, *J* = 8.0 Hz, 1 H), 8.63 (d, *J* = 7.0 Hz, 2 H), 9.14 (s, 1 H). – ^{13}C NMR (CD_3CN): δ = 25.4, 25.6, 29.4, 35.4, 37.7, 39.3, 41.1, 57.4, 116.7, 125.3, 126.2, 126.6, 128.6, 129.4, 130.3, 131.8, 132.0, 133.3, 133.5, 137.3, 141.9, 142.0, 148.3, 149.0, 150.1, 154.1, 154.4, 156.1, 157.8, 166.9, 174.3. – IR (KBr): ν(C=O) 1708, ν(C-C_{arom}) 1613, ν(C-N) + δ(N-H) 1507 cm^{-1}. – UV/Vis (CH_3CN): λ_{max} (ε in L mol^{-1} cm^{-1}) = 329 (9940), 360 (5880), 426 (2190) nm. – Emission (CH_3CN): λ_{max} = 556 nm (λ_{ex} = 425 nm). – MS ((+)-ESI): *m/z* = 784.4 (calcd. 784.2 for $C_{35}H_{33}N_4OPtS_2$, $[M]^+$). – Anal. for $C_{35}H_{33}N_4F_6OPPtS_2$ (929.8): calcd. C 45.21, H 3.58, N 6.03; found C 45.44, H 3.68, N 5.89.

Preparation of ***3****@GNP*

$H[AuCl_4]\cdot 3H_20$ (200 mg, 0.51 mmol) and [(*n*-$C_8H_{17})_4N$]Br (750 mg, 1.4 mmol) were dissolved in a mixture of water (25 mL) and toluene (40 mL). The mixture was stirred vigorously for 10 min, and **3** (282 mg, 1.00 mmol) was added. Stirring was continued for a further 10 min and the mixture cooled to 0 °C during this time. A freshly prepared ice-cold solution of $Na[BH_4]$ (190 mg, 5.00 mmol) in water (12.5 mL) was added dropwise to the stirred mixture over the course of 15 min. The stirred mixture was kept at 0 °C for another 30 min and was subsequently allowed to warm up to r. t. After 20 h the dark-violet organic layer was separated, and volatile components were removed *in vacuo*. The residue was dissolved in dichloromethane (20 mL). The product was precipitated by dropwise addition of *n*-hexane (50 mL) and collected by decanting. The precipitation procedure was repeated twice and the product finally isolated by filtration, which afforded a very dark, viscous paste. Yield 160 mg. – Particle size (TEM) (2.74 ± 0.78) nm. – ^{1}H NMR ($CDCl_3$): δ = 1.50 (m, 2 H), 1.71 (m, 4 H), 1.90 (m, 1 H), 2.41 (m, 3 H), 3.09 (m, 1 H), 3.14 (m, 1 H), 3.55 (m, 1 H), 7.03 (m, 1 H), 7.17 (m, 2 H), 7.25 (m, 2 H), 7.60 (m, 2 H). – IR: ν = 1675, 1599, 1545 cm^{-1}.

Preparation of ***4****@GNP*

$H[AuCl_4]\cdot 3H_2O$ (0.46 mg, 1.18 μmol), **4** (0.96 mg, 1.18 μmol) and *n*-octane thiol (0.17 mg, 1.18 μmol) were dissolved in CH_3CN (3 mL), and an aqueous solution of $Na[BH_4]$ (153 μL, 58 mM, 7.5 equiv.) was slowly added with constant stirring, which caused the solution to darken.

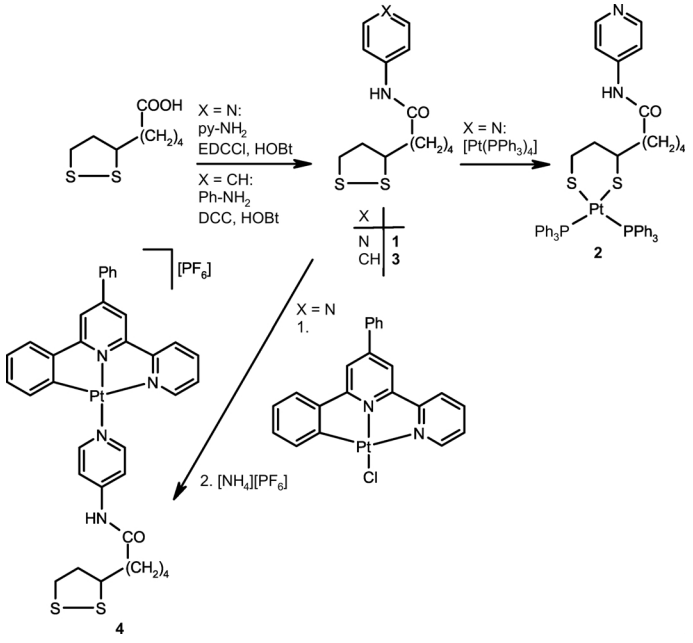

Scheme 1. New compounds prepared in this investigation.

After 5 min, this resulted in the slow formation of a black precipitate, which was collected after 30 min by centrifuge, washed copiously with CH_3CN and dried *in vacuo*. Yield 0.28 mg. – Particle size (TEM) (2.38 ± 0.67) nm. – Emission: λ_{max} (CH_2Cl_2, 298 K) = 546 (λ_{ex} = 300) nm. – IR (KBr): ν(C=O) ~1700 (vw), ν(C-C_{arom}) 1605, ν(C-N) + δ(N-H) 1477 cm^{-1}. – UV/Vis (aqueous acetonitrile): λ_{max} = 240, 279, 328, 360, 426, 540 (br.) nm.

Results and Discussion

Our strategy involves the attachment of luminescent Pt^{II} C^N^N chelates to gold nanoparticles. This can be achieved by a linker which contains terminal units suitable for (1) chemisorption on gold, and (2) binding suitable Pt^{II} luminophore fragments. Owing to our experience with α-lipoic acid (lip-COOH) derivatives for the fabrication of SAMs on gold [35, 36], we decided to utilise lip-C(O)NH-py (**1**) (py = pyrid-4-yl) as the linker component. The 1,2-dithiolane unit is excellently suited for chemisorption on gold, while the terminal pyridyl unit is known to readily coordinate $[Pt^{II}(C^N^N)]^+$ moieties [37, 38]. The synthesis of **1** was easily accomplished by the condensation of lip-COOH with $pyNH_2$ using the established peptide coupling reagent combination of *N*-ethyl-*N*'-(3-dimethylaminopropyl)carbodiimide hydrochloride (EDCCl) and 1-hydroxybenzotriazol (HOBt) in dichloromethane solvent (Scheme 1) [39 – 41].

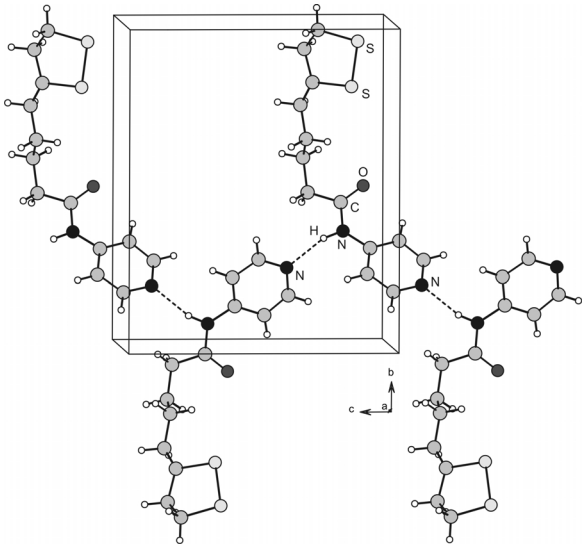

Fig. 2. Molecular structure and aggregation of **1** in the crystal.

The compound was structurally characterised by a single-crystal X-ray diffraction study (Fig. 2). Bond lengths and angles are unexceptional. While no amide C=O···H-N hydrogen bonds occur, N-H···py hydrogen bonds are observed between neighbouring molecules in the crystal, with parameters (N···N *ca.* 2.90 Å, N-H-N *ca.* 165°) in accord with a moderate bond strength [42]. Similar intermolecu-

lar N-H···py interactions have been observed previously [43].

The chemisorption of **1** on the surface of a gold nanoparticle is expected to occur by an oxidative addition of the 1,2-dithiolane unit to afford two thiolate-gold bonds [44], but a competing adsorption of the pyridyl moiety cannot be ruled out [45 – 47]. We have therefore reacted **1** with the zero-valent Pt complex $[Pt(PPh_3)_4]$ and found that an oxidative addition proceeded smoothly and swiftly at r. t., affording the Pt^{II} chelate **2** in good yield (Scheme 1). This lends further credence to the notion that **1** chemisorbs on gold by an oxidative addition of the S-S bond. The Pt^{II} chelate was structurally characterised by single-crystal X-ray diffraction (Fig. 3). Bond parameters compare well to those of closely related compounds [35, 48]. The Pt atom resides in a distorted square-planar coordination environment: the P-Pt-P and S-Pt-S angles are 97.6(2) and 93.2(2)°, respectively, while the two *cis*-P-Pt-S bond angles are 87.9(2) and 81.8(2)°, and the sum of angles around Pt is 360.5°. The Pt-P bond lengths [2.336(5) and 2.278(6) Å] and the Pt-S bond lengths [2.325(5) and 2.343(6) Å] differ only slightly. The molecules are aggregated as antiparallel dimers in the crystal, held together by intermolecular N-H···S interactions (N···S 3.39 Å, H···S 2.53 Å, N-H-S 166.1°) that correspond to hydrogen bonds of medium strength [49].

The assembly of three components is required in order to obtain gold nanoparticles functionalised with phosphorescent Pt complexes in the ligand shell, *viz.* the nanoparticle, the linker and a suitable Pt complex moiety. First of all, we have investigated the possibility to chemisorb the linker **1** on gold nanoparticles, in order to introduce the Pt^{II} component in the following step by chemical postmodification of the linker-containing nanoparticles. Two principal procedures are possible for the synthesis of such linker-containing gold nanoparticles, *viz.* by ligand substitution of preformed monolayer-protected nanoparticles or by direct synthesis. The direct synthesis involves the reduction of $H[AuCl_4]$ with $Na[BH_4]$ in the presence of an excess of **1**. We have followed the two-phase method (water/toluene solvent system, phase transfer catalyst) established by Brust *et al.* [50], using a protocol developed by Murray and coworkers [51]. Despite numerous attempts under various conditions of temperature, concentration and ratio of components, this approach did not afford soluble nanoparticles. Instead,

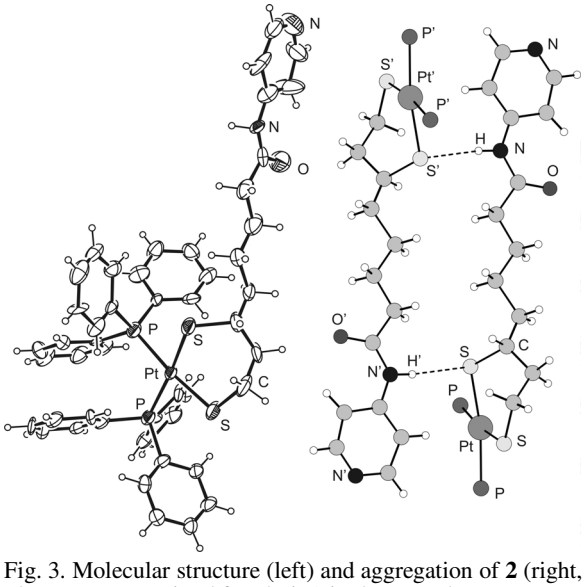

Fig. 3. Molecular structure (left) and aggregation of **2** (right, Ph groups are omitted for clarity) in the crystal.

an intractable black material was obtained which was completely insoluble in any solvent. When the reaction was performed in acetonitrile instead of a biphasic solvent system, similar results were obtained. The alternative ligand substitution approach was equally futile. We utilised triphenylphosphane-stabilised gold nanoparticles (Ph_3P@GNPs) obtained by the reduction of $[AuCl(PPh_3)]$ with B_2H_6 in toluene according to the protocol developed by Schmid [52], which in our hands afforded particles with a diameter of (1.77 ± 0.5) nm according to TEM analysis. A dichloromethane solution of these nanoparticles did not show the plasmon absorption band typical for larger (> *ca.* 2 nm) gold nanoparticles, which is located at *ca.* 520 nm [5]. Treatment of this solution with **1** at r. t. led to pronounced changes in the UV/Vis spectrum. A very broad band at *ca.* 670 nm was observed, typical for large aggregated or agglomerated particles [53], as subsequently corroborated by TEM analysis.

These results prompted us to study the role of **1** in more detail by performing similar experiments with its phenyl analogue lip-C(O)NH-Ph (**3**), which was synthesised by the condensation of lip-COOH with $PhNH_2$ using *N*,*N*′-dicyclohexylcarbodiimide (DCC) as coupling reagent (Scheme 1). By simple direct synthesis (Brust/Murray conditions) we were able to obtain soluble functionalised gold nanoparticles which were not prone to form larger aggregates. The presence of a weak surface plasmon band at 518 nm in

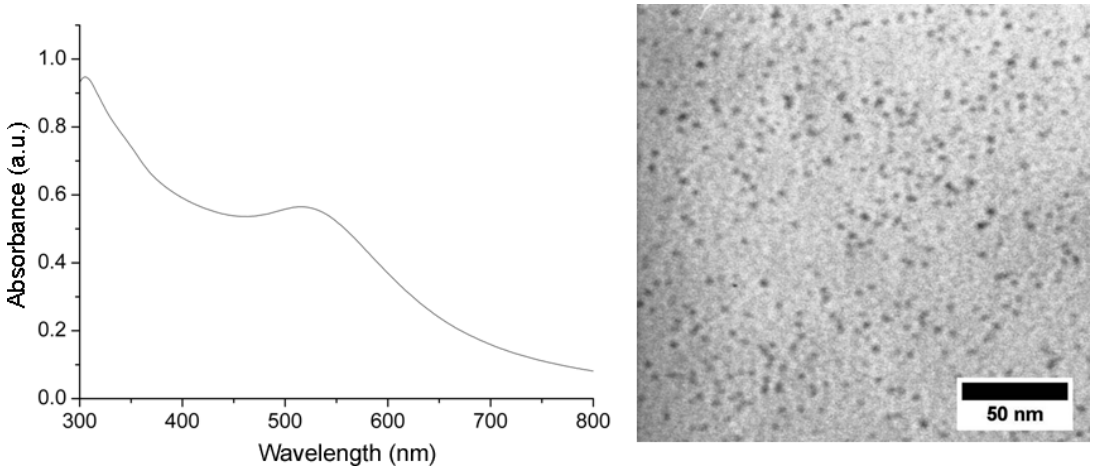

Fig. 4. UV/Vis spectrum (left; in toluene/H_2O) and TEM image (right) for gold nanoparticles functionalised with lip-C(O)NH-Ph (**3**) (**3**@GNP).

the UV/Vis spectrum indicated an average nanoparticle diameter between 2 and 3 nm, which is reassuringly compatible with the value of (2.74 ± 0.78) nm obtained from the TEM investigation (Fig. 4). The presence of substantial amounts of **3** chemisorbed on the nanoparticles was clearly evident from IR and ^{1}H NMR spectra. The fact that the use of the pyridyl-substituted α-lipoic acid derivative **1** did not allow the synthesis of soluble gold nanoparticles, but rather induced aggregation and agglomeration, can thus be attributed to the presence of the pyridyl group. This group may become engaged in substantial intermolecular hydrogen bonding, as is evident already from the crystal structure of **1** (*vide supra*). Intermolecular hydrogen bonds within or between monolayers may also constitute the main reason for our failure to prepare soluble gold nanoparticles with a ligand shell based on **1**.

The intended approach to chemisorb the linker **1** on gold nanoparticles in order to introduce the Pt^{II} component in the following step by chemical postmodification of linker-containing nanoparticles was evidently unsuccessful. We therefore turned our attention to the second approach based on the attachment of the Pt^{II} moiety to the linker **1** to afford an adsorbate species of the type $[Pt(\mathbf{1})(C^\wedge N^\wedge N)]^+$, which could be employed for chemisorption on a gold nanoparticle in the subsequent step. The reaction of **1** with the Pt^{II} complex $[PtCl(C^\wedge NPh^\wedge N)]$ was performed in a mixture of methanol and acetonitrile at reflux temperature, followed by anion metathesis, to give the target product $[Pt(\mathbf{1})(C^\wedge NPh^\wedge N)]PF_6$ (**4**, Scheme 1), which was characterised by ^{1}H and ^{13}C NMR spectroscopy, IR spectroscopy and ESI-MS.

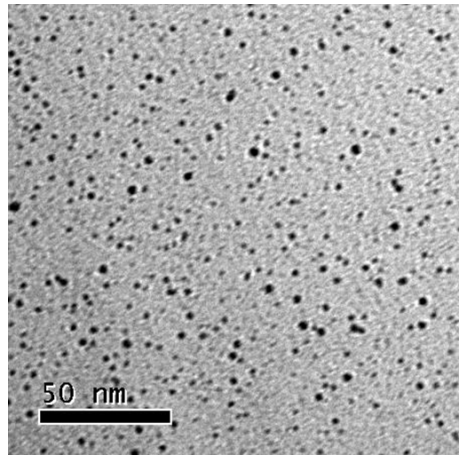

Fig. 5. TEM image for the product obtained from the reduction of $H[AuCl_4]$ with $Na[BH_4]$ in the presence of **4** and *n*-octane thiol.

The direct one-pot synthesis (reduction of $H[AuCl_4]$ with $Na[BH_4]$ in the presence of **4**) was performed in the presence of *n*-octane thiol to facilitate stabilisation of nanoparticles. A monophasic polar medium (aqueous acetonitrile) was chosen instead of the traditional biphasic water/toluene medium, because the ionic adsorbate species **4** exhibits reasonable solubility in polar organic solvents only. Due to the monophasic nature of the reaction, no transfer catalyst was required. The average diameter of the resulting nanoparticles turned out to be (2.38 ± 0.67) nm according to TEM analysis

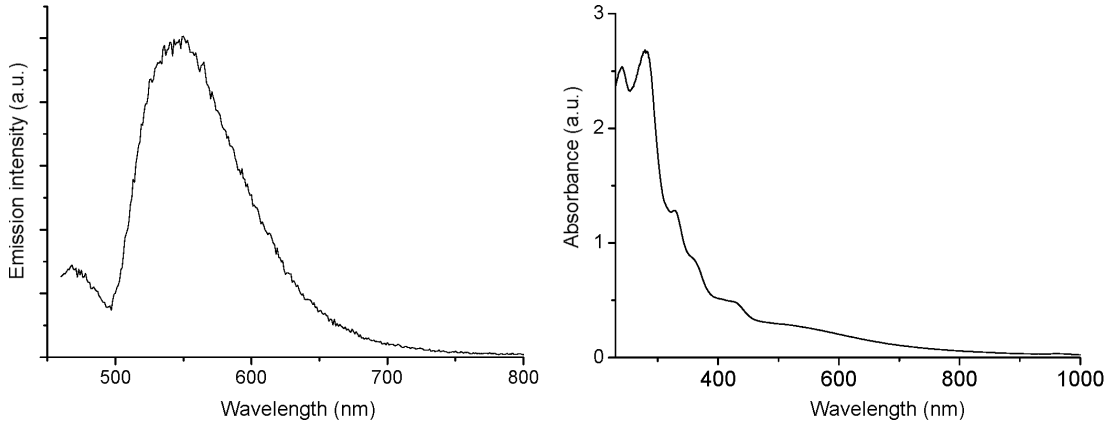

Fig. 6. Emission spectrum (left; in CH_2Cl_2 at 298 K, λ_{ex} = 300 nm) and UV/Vis spectrum (right; in aqueous acetonitrile) of the product obtained from the reduction of $H[AuCl_4]$ with $Na[BH_4]$ in the presence of **4** and *n*-octane thiol.

(Fig. 5), which is similar to the value of (2.74 ± 0.78) nm determined for **3**@GNP.

IR spectroscopic data are in accord with the presence of **4** chemisorbed on the nanoparticle surface. A ν(C-C_{arom}) band is located at 1605 cm^{-1}, which is close to the corresponding value of 1613 cm^{-1} observed for **4**. The ν(C-N) and δ(N-H) bands observed at 1507 cm^{-1} in the case of **4** have experienced a chemisorption-induced red shift of *ca.* 30 cm^{-1} and appear at the low end of the amide I region [54]. Not unexpectedly, the fairly weak intensity of the ν(C=O) band at 1700 cm^{-1} indicates an approximately orthogonal orientation of this moiety with respect to the surface normal according to the surface selection rule [55, 56]. The UV/Vis and emission spectra, too, are compatible with the presence of luminescent Pt-functionalised nanoparticles (Fig. 6). Future work will address the photophysical response of these nanoparticles towards suitable analytes which are prone to axial interaction with the square-planar Pt^{II} coordination environment.

Acknowledgements

The work described in this paper was supported by a travel grant from the Germany/Hong Kong Joint Research Scheme sponsored by the Research Grants Council of Hong Kong (Reference No. G_HK004/06) and the German Academic Exchange Service (DAAD, D/06 00385), and by a grant from City University of Hong Kong (7002130; for research activities performed in Hong Kong). We are grateful to Umicore AG & Co. KG (Hanau, Germany) for a generous gift of precious metal compounds. Prof. H. Zöltzer (Institute of Biology, University of Kassel) is thanked for recording the TEM images.

[1] M.-A. Neouze, U. Schubert, *Monatsh. Chem.* **2008**, *139*, 183 – 195.
[2] P. C. Chen, S. C. Mwakwari, A. K. Oyelere, *Nanotechn. Sci. Appl.* **2008**, *1*, 45 – 66.
[3] N. L. Rosi, C. A. Mirkin, *Chem. Rev.* **2005**, *105*, 1547 – 1562.
[4] E. Katz, I. Willner, *Angew. Chem.* **2004**, *116*, 6166; *Angew. Chem. Int. Ed.* **2004**, *43*, 6042 – 6108.
[5] M.-C. Daniel, D. Astruc, *Chem. Rev.* **2004**, *104*, 293 – 346.
[6] D. Astruc, M.-C. Daniel, J. Ruiz, *Chem. Commun.* **2004**, 2637 – 2649.
[7] Y.-S. Shon, H. Choo, *C. R. Chimie* **2003**, *6*, 1009 – 1018.
[8] J. H. Fendler, *Chem. Mater.* **2001**, *13*, 3196 – 3210.
[9] A. C. Templeton, W. P. Wuelfing, R. W. Murray, *Acc. Chem. Res.* **2000**, *33*, 27 – 36.
[10] J. D. E. T. Wilton-Ely, *Dalton Trans.* **2008**, 25 – 29.
[11] A. J. Hallett, P. Christian, J. E. Jones, S. J. A. Pope, *Chem. Commun.* **2009**, 4278 – 4280.
[12] E. R. Knight, N. H. Leung, Y. H. Lin, A. R. Cowley, D. J. Watkin, A. L. Thompson, G. Hogarth, J. D. E. T. Wilton-Ely, *Dalton Trans.* **2009**, 3688 – 3697.
[13] E. R. Knight, N. H. Leung, A. L. Thompson, G. Hogarth, J. D. E. T. Wilton-Ely, *Inorg. Chem.* **2009**, *48*, 3866 – 3874.
[14] E. R. Knight, A. R. Cowley, G. Hogarth, J. D. E. T. Wilton-Ely, *Dalton Trans.* **2009**, 607 – 609.

[15] C. R. Mayer, G. Cucchiaro, J. Jullien, F. Dumur, J. Marrot, E. Dumas, F. Sécheresse, *Eur. J. Inorg. Chem.* **2008**, 3614 – 3623.
[16] K. G. Thomas, P. V. Kamat, *Acc. Chem. Res.* **2003**, *36*, 888 – 898.
[17] K. G. Thomas, B. I. Ipe, K. P. Sudeep, *Pure Appl. Chem.* **2002**, *74*, 1731 – 1738.
[18] J. Massue, S. J. Quinn, T. Gunnlaugsson, *J. Am. Chem. Soc.* **2008**, *130*, 6900 – 6901.
[19] C. R. Mayer, E. Dumas, F. Sécheresse, *J. Colloid Interface Sci.* **2008**, *328*, 452 – 457.
[20] B. I. Ipe, K. Yoosaf, K. G. Thomas, *J. Am. Chem. Soc.* **2006**, *128*, 1907 – 1913.
[21] S.-W. Lai, C.-M. Che, *Top. Curr. Chem.* **2004**, *241*, 27 – 63.
[22] J. A. G. Williams, *Top. Curr. Chem.* **2007**, *281*, 205 – 268.
[23] K. M.-C. Wong, V. W.-W. Yam, *Coord. Chem. Rev.* **2007**, *251*, 2477 – 2488.
[24] C.-C. Kwok, S.-C. Yu, I. H. T. Sham, C.-M. Che, *Chem. Commun.* **2004**, 2512 – 2513.
[25] C.-M. Che, W.-F. Fu, S.-W. Lai, Y.-J. Hou, Y.-L. Liu, *Chem. Commun.* **2003**, 118 – 119.
[26] D.-L. Ma, C.-M. Che, *Chem. Eur. J.* **2003**, *9*, 6133 – 6144.
[27] C.-M. Che, J.-L. Zhang, L.-R. Lin, *Chem. Commun.* **2002**, 2556 – 2557.
[28] K. H. Wong, M. C. W. Chan, C.-M. Che, *Chem. Eur. J.* **1999**, *5*, 2845 – 2849.
[29] W. Lu, M. C. W. Chan, N. Zhu, C.-M. Che, C. Li, Z. Hui, *J. Am. Chem. Soc.* **2004**, *126*, 7639 – 7651, and refs. cited therein.
[30] S.-W. Lai, M. C.-W. Chan, T.-C. Cheung, S.-M. Peng, C.-M. Che, *Inorg. Chem.* **1999**, *38*, 4046 – 4055.
[31] S. Link, M. A. El-Sayed, *J. Phys. Chem.* B **1999**, *103*, 4212 – 4217.
[32] X-RED (version 1.06), Program for numerical absorption correction, Stoe & Cie GmbH, Darmstadt (Germany) **2004**.
[33] G. M. Sheldrick, SHELXS/L-97, Programs for Crystal Structure Determination, University of Göttingen, Göttingen (Germany) **1997**. See also: G. M. Sheldrick, *Acta Crystallogr.* **1990**, *A46*, 467 – 473; *ibid.* **2008**, *A64*, 112 – 122.
[34] C. K. Johnson, M. N. Burnett, ORTEP-3, Rep. ORNL-6895, Oak Ridge National Laboratory, Oak Ridge, TN (USA) **1996**. Windows version: L. J. Farrugia, University of Glasgow, Glasgow, Scotland (U. K.) **1999**. See also: L. J. Farrugia, *J. Appl. Crystallogr.* **1999**, *32*, 837 – 838.
[35] T. Weidner, F. Bretthauer, N. Ballav, H. Motschmann, H. Orendi, C. Bruhn, U. Siemeling, M. Zharnikov, *Langmuir* **2008**, *24*, 11691 – 11700.
[36] U. Siemeling, S. Rittinghaus, T. Weidner, J. Brison, D. Castner, *Appl. Surf. Sci.* **2010**, *256*, 1832 – 1836.
[37] D.-L. Ma, C.-M. Che, *Chem. Eur. J.* **2003**, *9*, 6133 – 6144.
[38] J. H. K. Yip, Suwarno, J. J. Vittal, *Inorg. Chem.* **2000**, *39*, 3537 – 3543.
[39] C. A. G. N. Montalbetti, V. Falque, *Tetrahedron* **2005**, *61*, 10827 – 10852.
[40] M. Bodanszky, A. Bodanszky, *The Practice of Peptide Synthesis*, Springer, Berlin, **1984**.
[41] W. König, R. Geiger, *Chem. Ber.* **1970**, *103*, 788 – 798.
[42] G. A. Jeffrey, *An Introduction to Hydrogen Bonding*, Oxford University Press, Oxford, **1997**.
[43] K. Donelly, J. F. Gallagher. A. J. Lough, *Acta Crystallogr.* **2008**, *C64*, o335 – o340.
[44] R. G. Nuzzo, D. L. Allara, *J. Am. Chem. Soc.* **1983**, *105*, 4481 – 4483.
[45] B. C. Barlow, I. J. Burgess, *Langmuir* **2007**, *23*, 1555 – 1563.
[46] A. Bilić, J. R. Reimers, N. S. Hush, *J. Phys. Chem. B* **2002**, *106*, 6740 – 6747.
[47] L. Stolberg, S. Morin, J. Lipkowski, D. E. Irish, *J. Electroanal. Chem. Interfac. Electrochem.* **1991**, *307*, 241 – 242.
[48] S. M. Aucott, H. L. Milton, S. D. Robertson, A. M. Z. Slawin, G. D. Walker, J. D. Woollins, *Chem. Eur. J.* **2004**, *10*, 1666 – 1676.
[49] U. Siemeling, F. Bretthauer, C. Bruhn, *Z. Anorg. Allg. Chem.* **2006**, *632*, 1027 – 1032, and refs. cited therein.
[50] M. Brust, M. Walker, D. J. Schiffrin, R. Whyman, *J. Chem. Soc., Chem. Commun.* **1994**, 801 – 802.
[51] M. J. Hostetler, J. E. Wingate, C.-J. Zhong, J. E. Harris, M. R. Clark, J. D. Londono, S. J. Green, J. J. Stokes, G. D. Wignall, G. L. Glish, M. D. Porter, N. D. Evans, R. W. Murray, *Langmuir* **1998**, *14*, 17 – 30.
[52] G. Schmid, *Inorg. Synth.* **1990**, *27*, 214 – 218.
[53] C. S. Weisbecker, M. V. Merritt, G. M. Whitesides, *Langmuir* **1996**, *12*, 3763 – 3772.
[54] F. Fillaux, J. P. Fontaine, M.-H. Baron, G. J. Kearley, J. Tomkinson, *Chem. Phys.* **1993**, *176*, 249 – 278.
[55] J. T. Young, F. J. Boerio, Z. Zhang, T. L. Beck, *Langmuir* **1996**, *12*, 1219 – 1226.
[56] M. K. Debe, *J. Appl. Phys.* **1984**, *55*, 3354 – 3366.